

# Physics based Degradation Modeling and Prognostics of Electrolytic Capacitors under Electrical Overstress Conditions

Chetan S. Kulkarni \*

*SGT Inc., NASA Ames Research Center, Moffett Field, CA, 94035*

José R. Celaya †

*SGT Inc., NASA Ames Research Center, Moffett Field, CA, 94035*

Gautam Biswas ‡

*Institute for Software Integrated Systems (ISIS), Vanderbilt University, Nashville, TN, 37235*

Kai Goebel §

*NASA Ames Research Center, Moffett Field, CA, 94035*

**This paper proposes a physics based degradation modeling and prognostics approach for electrolytic capacitors. Electrolytic capacitors are critical components in electronics systems in aeronautics and other domains. Degradations in capacitor and MOSFET components are often the cause of failures in DC-DC converters. For example, prevalent fault effects, such as a ripple voltage surge at the power supply output, can damage interconnected critical subsystems leading to cascading fault propagation. Prognostics in general and in this case electronics components in particular is concerned with the prediction of remaining useful life (RUL) of components and systems. It performs a condition-based health assessment by estimating the current state of health. Furthermore, it leverages the knowledge of the device physics and degradation physics to predict remaining useful life as a function of current state of health and anticipated operational and environmental conditions. Physics-based models capture degradation phenomena in terms of component geometry and energy based principles that define the effect of stressors on the component behavior. This is in contrast to the traditional approach for deriving degradation models from empirical data. Implementing the degradation modeling techniques present a general methodology for estimating lifetimes due to specific failure mechanisms. The failure rate models can be tuned to include parameters that relate to the present health of the device/system and the expected conditions under which it will be operated. The models and algorithms are applied to data from degradation experiments of several COTS capacitors. Results show the efficiency of the approach chosen.**

## Nomenclature

$\epsilon_R$	relative dielectric constant
$\epsilon_O$	permittivity of free space
$A_s$	effective oxide surface area,
$c_b$	capacitance dependence breakdown factor.
$V_{e(t)}$	dispersion volume at time $t$
$V_{e0}$	initial electrolyte volume
$j_{eo}$	evaporation rate ( $min^{-1} area^{-1}$ )

---

\*Research Engineer II, Prognostics Center of Excellence and AIAA Member.

†Research Scientist, Prognostics Center of Excellence and AIAA Member.

‡Professor, Electrical Engineering and Computer Science, Institute for Software Integrated Systems

§Deputy Area Lead for Discovery and System Health and AIAA Senior Member.

$t$	aging time in hours
$\rho_E$	electrolyte resistivity
$P_E$	correlation factor related to electrolyte spacer porosity and average electrolyte path.
$w_e$	volume of ethyl glycol molecule
$V_c$	total capacitor capsule volume
$d_A$	thickness of anode strip
$d_C$	thickness of cathode strip
$C$	Capacitance

## I. Introduction

Today almost all of the sub-systems in a complex system include modules with embedded electronics to carry out a variety of different tasks. However, it has been found that these modules are often the first elements in the system to fail thus reducing overall system reliability.<sup>1,2</sup> These failures can often be attributed to adverse storage and operating conditions, such as high temperatures, voltage surges and current spikes that the modules and their components may be subjected to during operation. This motivates the need for developing and implementing Integrated Vehicle Health Management (IVHM) technologies for systems with embedded electronics to enhance system reliability, assure system performance, avoid catastrophic failures, and reduce maintenance costs over the life of the system.<sup>3,4</sup> In addition, an understanding of the deterioration mechanisms helps to systematically track the changes in system behavior and performance, develop the capability to anticipate failures, and predict the remaining useful life (RUL) of the electronic systems long before the components actually fail.

The term “diagnostics” relates to the ability to detect and isolate faults or failures in a system. “Prognostics” on the other hand is the process of predicting health condition and remaining useful life based on current state and previous, current and future operating conditions. Prognostics and health management (PHM) methods combine sensing, data collection, interpretation of environmental, operational, and performance related parameters to indicate systems health as well as anticipate damage propagation due to degradation. PHM methodologies can be implemented through the use of various techniques that study parameter variations, which indicate changes in performance degradation based on usage duration and conditions.

In this paper, we develop an effective PHM methodology to enable early detection of failure precursors in a specific type of electrolytic capacitor associated with DC-DC power supplies. Our approach combines physics-based degradation modeling supported by empirical experimental analysis for parameterizing the physics models, and then using these models to predict remaining useful life of electrolytic capacitors as well as their effects on overall system performance. Our hypothesis is that early detection will lead to better tracking of the degradation process, thus enabling better predictions and end of life estimates. As a result, this will result in better overall performance and system reliability. The overall contribution of this paper is the development of a mixed physics-based and data-driven methodology, and demonstration of how it applies to modeling the degradation process and RUL in one type of capacitor. We believe that the methodology is general, and may be extended to structurally similar type of capacitors. We hope to demonstrate that in future work.

### A. Background

We study and analyze an example from the aerospace domain, where flight and ground staff need to acquire relevant information that enables accurate estimation of the current health state for all subsystems. Avionics systems in modern aircraft contain a large number of electronics components in the control, communications and navigation systems. Furthermore, with the introduction of fly-by-wire mechanisms, the number of electronic components in aircraft systems are growing. This proliferation gives rise to the possibility of unknown fault modes, which will affect the ability to detect and diagnose faults in a robust and computationally efficient ways. This increases the importance of understanding how these components degrade, and to use this understanding to anticipate, track, isolate, identify, and predict the remaining useful life of the electronic components.<sup>3,5</sup> This has motivated research projects that focus on accurate detection and isolation of degradation and faults in the system, develop precursors to failure, and predict remaining useful life of the critical avionics components and subsystems after degradation or onset of faults have been detected.

Capacitors are an integral components of switched-mode power supplies that are used in a number of aircraft systems because of their high efficiency and compact size. The buck-boost DC-DC converter steps voltage levels

down/up based on the application requirements. Our particular application has an input of 28V DC from a battery source, and the required output voltage of 5V. The electrolytic capacitors and metaloxide semiconductor field-effect transistor (MOSFET) switches are known to have the highest degradation and failure rates among all of the components.<sup>6</sup> Degraded capacitors affect the performance and efficiency of the DC-DC converters in a significant manner and also impose a risk on instantiating cascading failures on other connected subsystems.

Some earlier efforts in diagnostic health monitoring of electronic systems and subsystems involved the use of a built-in test (BIT), defined as an on-board hardware-software diagnostic tests to identify and locate faults. Studies conducted by<sup>7,8</sup> on the use of BITs for fault identification and diagnostics showed that they can be prone to false alarms and may result in unnecessary costly replacement, re-qualification, delayed shipping, and loss of system availability. The persistence of such issues over the years is perhaps because the use of BIT has been restricted to low-volume systems. In general, BITs generally have not been designed to provide prognostics or remaining useful life due to accumulated damage or progression of faults. Rather, it has served primarily as a diagnostic tool.

Prognostics failure predictions have to be accurate if they are used in taking decisions for reliability improvement and repair. Detailed examinations of actual parameter variations and degradation process should also be compared with those that are predicted by the physics-based failures models. Between similar components or electronic systems, (made by different manufacturers) there may be wide variability in the parameters values and hence making effective predictions based on specific data set.<sup>9</sup> Hence implementing PHM methodology based on first principles of operation is highly effective and efficient in making remaining useful life predictions under such circumstances.

## **B. Organization of Paper**

This paper is organized as follows. Section II discusses the current work being done in the area of capacitor prognostics and our research approach. Section III presents introduction to electrolytic capacitors and its basic structure, operation and degradation mechanisms. Section IV discusses capacitor first principle models in detail. Section V describes the electrical overstress aging experiments conducted for this work. Section VI and VII presents the prognostic framework methodology and RUL results respectively. The paper ends with discussion and conclusion in section VIII.

## **II. Related Work in Capacitor Diagnosis and Prognosis**

The high frequency of failure of the output filter capacitor in switched mode power supplies has a critical impact on overall system performance and reliability.<sup>6,10,11</sup> A PHM approach applied to power supplies used in avionics systems is presented in,<sup>11</sup> where aging of the system is attributed to output capacitor and power MOSFET degradation and failures. However, the paper does not discuss the degradation processes or a methodology to derive RUL predictions for the power supply. The work on switched mode power supplies by<sup>6,10</sup> discuss details of the power supply output ripple voltage and leakage current as a function of capacitor degradation, but they do not discuss modeling of the degradation mechanisms and RUL computations in any detail.

A health management approach for multilayer ceramic capacitors is presented in.<sup>12</sup> This approach focuses on a temperature-humidity bias accelerated test to replicate failures, and implements data trending algorithms in conjunction with multivariate data analysis. The Mahalanobis distance method is used to detect abnormalities in the data by using classification methods that label behaviors into “normal” and “abnormal” groups. The abnormal data are then further classified into levels of abnormality by severity based on which predictions are made. A data driven fault detection and prediction algorithm for multilayer ceramic capacitors is presented in.<sup>13</sup> The prediction approach used in their study combines regression analysis, residual, detection, and prediction analysis. A method based on Mahalanobis distance is used to detect abnormalities in the test data; prediction of RUL is not discussed in this paper.

The authors in<sup>14</sup> discuss the failure probability in Barium Titanate used as a dielectric in MLCC's. Dielectric ceramics in multilayer capacitors are subjected to thermo-mechanical stresses, which, may cause mechanical failure and lead to loss of electrical function. Probabilistic life design or failure probability analysis of ceramic components combines the strength distribution of the monolithic ceramic material comprising the component, finite element analysis of the component under the mechanical loading conditions of interest, and a multiaxial fracture criterion.

The work by<sup>15</sup> looked at degradation in metalized polypropylene film capacitors, where a noninvasive technique for capacitor diagnostics in boost converters has been discussed. This technique is based on estimations of the ESR (equivalent series resistance) and the capacitance, improving the diagnostic reliability and allowing for predictive maintenance using a low-cost digital signal processor.<sup>16</sup> discuss a condition based monitoring with implementation of fast fourier transform based prediction approach.

Most of the current work done for capacitor prognostics is based on data driven methodologies. As discussed

earlier<sup>12</sup> implement a trending algorithm based on experimental data, similarly<sup>13</sup> implemented a data driven fault detection and prediction algorithm. In this work we discuss implementation of an hybrid approach, combining data driven and physics based degradation modeling approaches for prognostics.

### A. Research Approach

The physics-based degradation modeling (PBDM) approach to prognosis, models failure mechanisms using a first principles physics-based model of operation, as opposed to traditional approaches that employ data-driven empirical models. These are dynamic models which evolve over time as the device/ system degrades due to usage conditions. Physics-based degradation modeling techniques are effective for estimating the impact on lifetime due to specific failure mechanisms.<sup>17</sup> Failure predictions, i.e., the time to complete failure from the present time (RUL) and also the evolution of degradation through this time interval, depend upon the current health state of the device/system and the conditions under which it is operated. Therefore, to apply PBDM techniques accurately, one must take into account environmental variables and operating conditions along with a device’s physical properties.

Typically, under normal operating conditions, where parameters are limited to manufacturer-specified threshold limits, a device/ subsystem does not degrade rapidly. In such cases, an experiment may have to be conducted over long periods of time (e.g., months and even years) to detect and study the underlying failure modes. Accelerated stress tests (AST) have been recognized to be a valuable in getting much quicker estimates of the reliability and quality of electronics components.<sup>17</sup> Accelerated stress tests are often carried out under enhanced adverse environmental conditions to accelerate the damage accumulation rate due to physical or environmental phenomena.<sup>18</sup> In traditional accelerated testing techniques, root-cause identification and analysis is not adequately emphasized. In the physics-based degradation modeling (PBDM) approach it is very important to identify, understand, and model the underlying failure mechanisms to derive general (as opposed to situation-specific) models of the aging phenomena.

As mentioned earlier, prognostics approaches are essential for improving system safety, reliability, and availability. Prognostics deals with determining the health state of components, and projecting this state into the future to make end of life (EOL) and RUL estimations. Model-based prognostics approaches perform these tasks employing first principles physics models that capture knowledge about the system, its components, and their degradation mechanisms.<sup>19</sup> Faults and degradations appear as parameter value changes in the model, and this provides the mechanism for tracking system behavior under degraded conditions.<sup>20</sup>

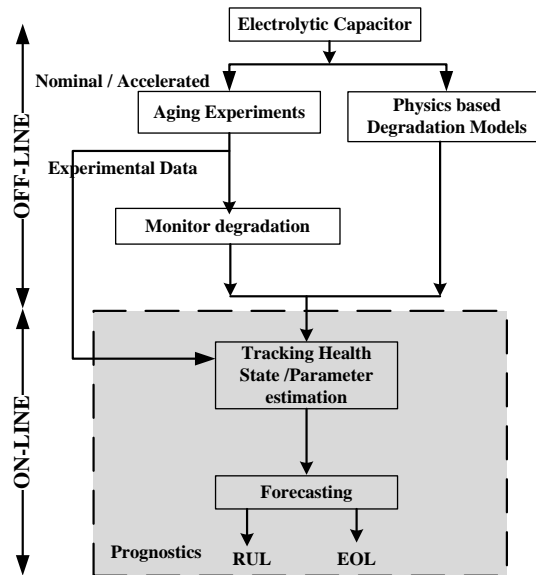


Figure 1. Research Approach Methodology

We implement the prognostics modeling process illustrated in Figure 1. The core of this work focuses on developing physics-based degradation models of components that include descriptions of how fault parameters evolve in time, governed by their operating conditions. As described in Figure 1, we combine experimental studies on the device and the electrical and mechanical configuration information with physics based modeling of behavior phenomena. Identifying the failure precursors and developing accurate models of degradation/ failure from an understanding of

the physics-based model is an important challenge that we address in this research work. Early detection and analysis may lead to more accurate estimation of parameter changes, and therefore, better prediction and end of life estimates of the capacitor. Unknown and time varying parameters in the degradation model are estimated online. The derived state space models are then implemented in a Bayesian framework for prognostics.

In the next section we first discuss in brief the basics of electrolytic capacitors, their detailed structure and the different mechanisms under which the devices degrade.

### III. Electrolytic Capacitors

Electrolytic capacitor performance is strongly affected by its operating conditions, such as voltage, current, frequency, and ambient temperatures. A primary reason for wear out in aluminum electrolytic capacitors is due to vaporization of electrolyte and degradation of electrolyte due to ion exchange during charging/discharging, which in turn leads to a drift in the two main electrical parameters of the capacitor: (1) the equivalent series resistance (*ESR*), and (2) the capacitance (*C*). The *ESR* of a capacitor is the sum of the resistance due to aluminum oxide, electrolyte, spacer, and electrodes (foil, tabbing, leads, and ohmic contacts)<sup>21</sup> and capacitance is the ability of a capacitor to store charge in an electric field. The health of a capacitor is often measured by the values of these two parameters. There are certain industry standard thresholds for these parameter values, if the measurements exceed these thresholds then the component is considered unhealthy, i.e., the component has reached its end of life, and should be immediately replaced before further operations.<sup>22,23</sup>

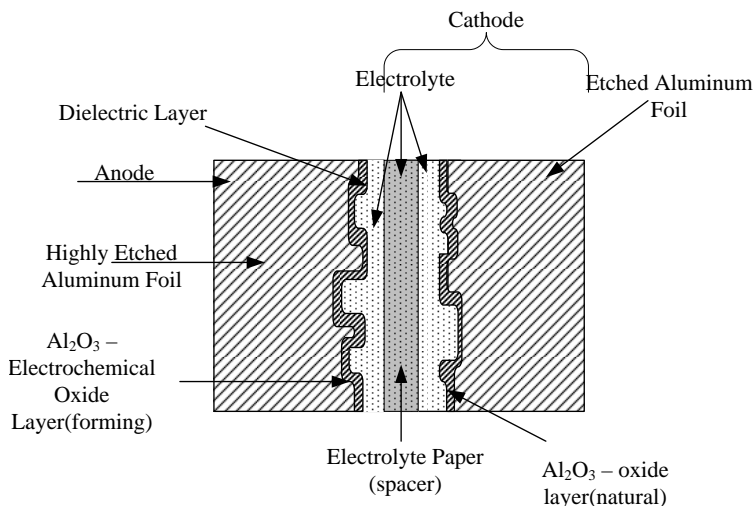


Figure 2. Capacitor Detail Structure

Fig. 2 shows a detailed view of the cross section of an electrolytic capacitor structure along with its equivalent electrical circuit diagram. Further details of the structure of a capacitor are discussed in <sup>21</sup>. To get higher capacitance values for the same surface area of the anode and cathode foils, the foil is etched by a chemical process. After etching, the plates are anodized by coating them with a thin aluminum oxide layer on the surface of the foil.

#### A. Degradation Mechanisms

There are several factors that cause degradation in electrolytic capacitors. Failures in a capacitor can be one of two types: (1) catastrophic failures, where there is complete loss of functionality due to a short or open circuit, and (2) degradation failures, where there is gradual deterioration of capacitor due to accumulated damages. Degradation in the capacitor manifests an increase in the equivalent series resistance (*ESR*) and decrease in capacitance (*C*), due to deterioration of electrolyte quality, decreases in electrolyte volume due to evaporation, weakening of the oxide layer, over operating time.<sup>21,24</sup>

The flow of current during the charge/ discharge cycle of the capacitor causes the internal temperature to rise. The heat generated is transmitted from the core to the surface of the capacitor body, but not all the heat generated can escape. The excess heat results in a rise in the internal temperature of the capacitors which causes the electrolyte to evaporate, and gradually deplete. Similarly in situations where the capacitor is operating under high temperature

conditions, the capacitor body is at a higher temperature than its core, the heat travels in the opposite directions from the body surface to the core of the capacitor again increasing the internal temperature causing the electrolyte to evaporate.<sup>21</sup>

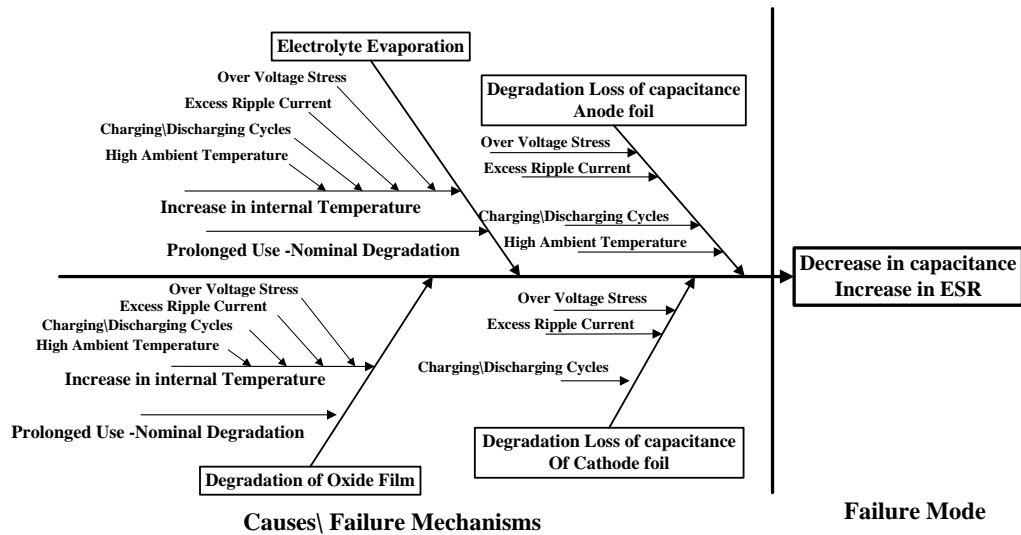


Figure 3. Fishbone diagram of failure mechanisms in aluminum electrolytic capacitors

Degradation in the oxide layer can be attributed to crystal defects that occur because of the periodic heating and cooling during the capacitor’s duty cycle, as well as stress, cracks, and installation-related damage. High electrical stress is known to accentuate the degradation of the oxide layer due to localized dielectric breakdowns on the oxide layer.<sup>25</sup> These breakdowns, which accelerate the degradation, have been attributed to the duty cycle, i.e., the charge/discharge cycle during operation.<sup>21</sup> Further another simultaneous phenomenon is the increase in the internal pressure due to an increased rate of chemical reactions,<sup>21</sup> which can again be attributed to the internal temperature increase in the capacitor. This pressure increase can ultimately lead to the capacitor popping open at the top.

All the failure/degradation phenomenon mentioned may act simultaneously based on the operating conditions of the capacitors. We first study the phenomenon qualitatively, and then discuss the steps to derive the first principles analytic degradation models for the different operating condition. The fishbone diagram in Fig. 3 shows the most common set of failure modes for electrolytic capacitors that have been reported in the literature.<sup>21</sup> This diagram identifies the relationship between root causes and failure modes observed in electrolytic capacitors. Our focus in this work is on the electrical stressors that govern the capacitor degradation, specifically, we study the effect of high operating voltage and their effects on the electrolytic capacitor degradation.

#### IV. Physics based Modeling of Capacitor Degradation

In this section we discuss about deriving the first principles based degradation models. We derive the capacitance and ESR degradation models which are based on the first principles of operation based on the first principles of operation and geometry.<sup>21</sup>

##### A. Electrolyte Decrease

The evaporation rate,  $j_{eo}$  is directly linked with change in the core temperature.<sup>26</sup> In this work the electrolyte under study is ethylene glycol. When the surrounding temperature of the capacitor capsule is high, heat transfer from the capsule to the capacitor core causes the internal temperature of the capacitor to increase, and as a result the electrolyte evaporates at a faster rate. Under prolonged high temperate exposure the electrolyte evaporation accelerates, which in turn decreases effective oxide surface area  $A_s$ , leading to decreases in capacitance,  $(C)$ .<sup>26-28</sup> The change in electrolyte volume as a function of the evaporation rate and time elapsed is given by:

$$V_e(t) = V_{e0} - (A_s j_{eo} w_e \times t), \quad (1)$$

From Eqn.(1) we derive the effective oxide surface areas  $A_s$  in terms of the decrease in electrolyte volume over time:

$$A_s = \frac{V_{e0} - V_e(t)}{j_{eo} t e} \quad (2)$$

Details of the derivation of this equation can be found in.<sup>21,26</sup>

## B. Capacitance Degradation Model

Capacitance represents the ability of a body to store electrical charge. It can be calculated from knowledge of the configuration and the geometry of the conductors and dielectric properties of the insulator between the conductors. Based on the cylindrical geometry the total lumped capacitance for a foil type electrolytic capacitor<sup>29</sup> along with capacitance dependence factor  $c_b$ , is given by:

$$C = \frac{2\epsilon_R\epsilon_0 A_s c_b}{d_C} \quad (3)$$

Studies reported in the literature<sup>30</sup> and our own experiments show that this parameter in the initial life aging cycle of the device remains less dominant based on the operating conditions and is directly proportional to decrease in electrolyte as discussed earlier. In Eq. (3) the parameters  $\epsilon_R$ ,  $\epsilon_0$ , and  $d_C$  remain more or less constant through the capacitance aging time.

## C. ESR Degradation Model

The *ESR* dissipates some of the stored energy in the capacitor. An ideal capacitor would offer no resistance to the flow of current at its leads. Based on the first principles parameters the equivalent series equivalent resistance, *ESR* is computed as a function of the effective oxide surface area,  $A_s$ <sup>29</sup> and the resistance dependence factor  $e_b$  can be expressed as:

$$ESR = \frac{1}{2} \left( \frac{\rho_E d_C P_E e_b}{A_s} \right) \quad (4)$$

Under normal circumstances when the capacitors are stored at room temperature or below rated temperatures, no significant damage or decrease in the life expectancy is observed for long periods of time. But in cases where the capacitors are stored under temperature conditions higher than their rated value, the capacitors show irreversible degradation over time. For both the capacitance and degradation models, we employ derived relation between, oxide surface area,  $A_s$  and electrolyte volume,  $V_{e(t)}$  to define temporal degradation in the  $C$  and *ESR* values when stress is applied.

## D. Time Dependent Degradation Models

Using the physics-based model of electrolyte evaporation, we derive the time dependent degradation models for capacitance ( $C$ ) and *ESR*. Using Eq. (3) and Eq. (2) we derive the *capacitance degradation model* as:

$$\mathcal{D}_1 : C(t) = \left( \frac{2\epsilon_R\epsilon_0 c_b}{d_C} \right) \left( \frac{V_e(t)}{j_{eo} t w_e} \right). \quad (5)$$

Evaporation rate,  $j_{eo}$  is a temperature dependent parameter, electrolyte volume changes with time and evaporation rate and  $c_b$  is the breakdown capacitance dependence factor directly dependent on the change in electrolyte volume. Similarly increase in *ESR*, is computed from Eq. (4) as:

$$\mathcal{D}_2 : ESR(t) = \frac{1}{2} (\rho_E d_C P_E) \left( \frac{j_{eo} t w_e e_b}{V_e(t)} \right) \quad (6)$$

In model,  $\mathcal{D}_2$  the parameters which are temperature dependent are the rate of evaporation  $j_{eo}$  and the correlation factor,  $P_E$  related to electrolyte spacer porosity and average liquid pathway and  $e_b$ , breakdown resistance dependence factor directly dependent on the change in electrolyte volume, operating conditions.

## V. Electrical Overstress Experiment

For this experiment six capacitors of  $2200\mu\text{F}$  capacitance, with a maximum rated voltage of  $10\text{V}$ , maximum current rating of  $1\text{A}$  and maximum operating temperature of  $85^\circ\text{C}$  were used for the study. The ESR and capacitance values were estimated from the capacitor impedance frequency response measured using the EIS instrument. Using the lumped parameter model,  $\mathcal{M}_1$  the ESR and capacitance ( $C$ ) values given by Eqns. (5) and (6), were estimated at each measurement. The average pristine condition ESR value was measured to be  $0.121\ \Omega$  and average capacitance of  $2029\ \mu\text{F}$  for the set of capacitors under test. The ambient temperature for the experiment was controlled and kept at  $25^\circ\text{C}$ . During each measurement the voltage source was shut down, the capacitors were discharged completely, and then the characterization procedure was carried out. Figure 4 shows the experimental setup for the  $15\text{V}$  EOS experiment.

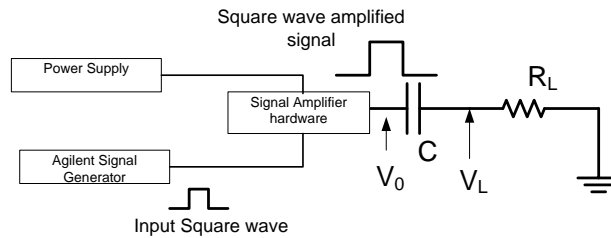


Figure 4. Electrical Overstress experimental setup schematic

Figure 5 shows increase in the ESR value for all the six capacitors under test over the period of time. Similarly, Figure 6 shows the decrease in the value of the capacitance as the capacitor degrades over the aging period. From the plots in Figure 5 we observe that for the time for which the experiments were conducted the average ESR value increased by  $54\% - 55\%$  while over the same period of time, the average capacitance decreased by more than  $20\%$  (threshold mark for a healthy capacitor). We used the collected data from the experiments to build dynamic degradation models of capacitors.

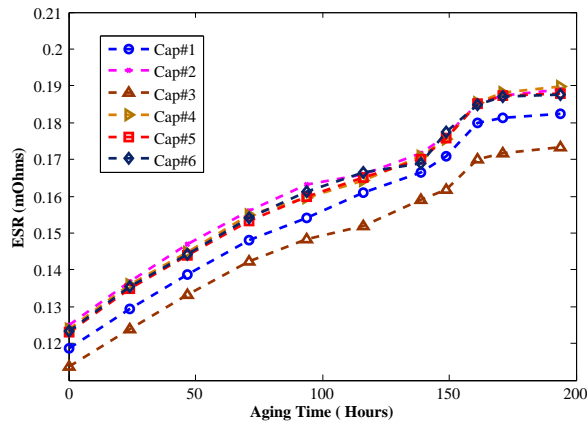


Figure 5. Degradation of capacitor performance, ESR increase as a function of aging time.

## VI. Model-based Prognostics Framework

In our earlier work<sup>20,31</sup> an implementation of a model-based prognostics algorithm based on Kalman filter (KF) and a physics inspired empirical degradation model has been presented. The physics inspired degradation model was derived based on the capacitance degradation data from electrical overstress experiments. In<sup>21</sup> we discussed an extension of our work where a physics based degradation model was derived and implemented for making RUL predictions for degradation under thermal overstress conditions. In this section we present our work extending it to the electrical overstress conditions and with implementation of the Bayesian framework methodology for prognostics<sup>19</sup> using an Unscented Kalman Filter (UKF).<sup>32</sup>

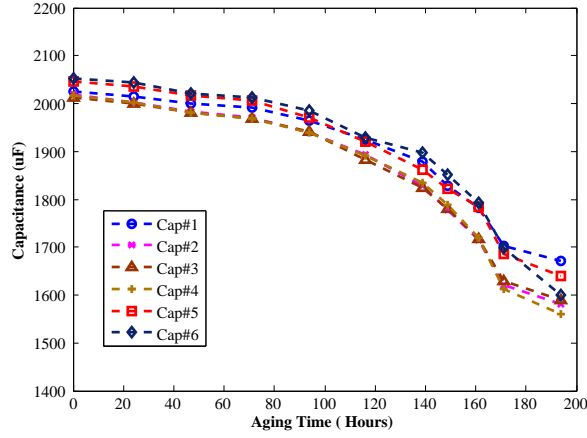


Figure 6. Degradation of capacitor performance, capacitance loss as a function of aging time.

### A. Prognostics Problem Formulation

In prognostics studies, it is important know when the performance of the device or system is going to lie outside an acceptable region of operation. When the capacitor parameters exceed specified thresholds, we consider the degrading device or system to have failed. For the device/system to be within the bounds of acceptable performance, we express a set of constraints,  $c_n$ ,  $\mathcal{C} = \{C_i\}_{i=1}^{c_n}$ , where  $C_i$  is a function

$$C_i : \mathbb{R}^{n_x} \times \mathbb{R}^{n_\theta} \rightarrow \mathbb{B}$$

that maps a given point in the joint state-parameter space,  $(x(t), \theta(t))$ , to the Boolean domain  $\mathbb{B} = [0, 1]$ , where  $C_i(x(t), \theta(t)) \triangleq 1$  indicates the constraint is satisfied or 0 (failed) if the constrained is not satisfied. Each individual constraint can be combined to form a single constraint output threshold function  $T_{EOL}$ , where

$$T_{EOL} : \mathbb{R}^{n_x} \times \mathbb{R}^{n_\theta} \rightarrow \mathbb{B}$$

which is defined as :

$$T_{EOL}(x(t), \theta(t)) = \begin{cases} 1, & 0 \in \{C_i(x(t), \theta(t))\}_{i=1}^c \\ 0, & \text{otherwise.} \end{cases} \quad (7)$$

Indicating the healthy state of a device/system  $T_{EOL}$  evaluates to 1, if any of the constraints are violated. At some instance in the aging cycle at time,  $t_p$ , the system is at  $(x(t_p); \theta(t_p))$  and we are interested in predicting the time point  $t$  at which this state will evolve to  $(x(t); \theta(t))$  such that  $T_{EOL}(x(t), \theta(t)) = 1$ . Using  $T_{EOL}$ , we formally define end of life (EOL) of a device/system as:

$$EOL_{t_p} \triangleq \inf \{t \in \mathbb{R} : t \geq t_p \wedge T_{EOL}(x(t), \theta(t)) = 1\}, \quad (8)$$

i.e.,  $EOL$  is the earliest instance in the aging cycle at which at which  $T_{EOL}$  is valid for a healthy system. RUL is expressed using  $EOL$  as

$$RUL(t_p) \triangleq EOL(t_p) - t_p.$$

### B. Capacitance Degradation Dynamic Model

From Eqn.(5) and other derivations derived earlier, we have the time dependent degradation model,  $\mathcal{D}_1$  for capacitance ( $C$ ) given by :

$$\mathcal{D}_1 : C(t) = \left( \frac{2 \epsilon_R \epsilon_0 c_b}{d_C} \right) \left( \frac{V_{e0} - V_e(t)}{j_{eo} t w_e} \right),$$

The degradation in capacitance is directly proportional to the damage variables  $V$  and  $c_b$ , respectively. The resultant decrease in the capacitance can be computed using Eq. (5). In addition to the decrease in electrolyte volume, the oxide layer also degrades causing a breakdown in the oxide layer, which further leads to degradation in capacitance ( $C$ ) and  $ESR$ .

In model,  $\mathcal{D}_1$  the parameters which are temperature dependent are the rate of evaporation  $j_{eo}$  and oxide breakdown factor,  $c_b$ . Rate of evaporation,  $j_{eo}$  and resistance dependence oxide breakdown factor,  $c_b$  are the two parameters in the model which are estimated online based on the state variable value,  $C$ .

Though the applied stress conditions are similar, there may be variation in each capacitor and hence each capacitor may have slightly different evaporation rate. Hence the evaporation rate parameter,  $j_{eo}$  is estimated based on the first two reading in the experimental data for each capacitors when predictions are done. The exact formulation of the parameter is incorporated as modeling error/process noise in form of a stochastic process. Since there could be a variation in the temperature the corresponding evaporation rate value estimated had a mean and variance of the variation values.

The complete discrete time dynamic model for capacitance degradation and state parameter, capacitance dependence breakdown factor,  $c_b$  can be expressed as:

$$\begin{aligned} \mathcal{D}_4 : C_{k+1} &= C_k - \frac{(2\epsilon_R \epsilon_0 w_e A_s j_{eo} c_b)}{d_C^2} \Delta t, \\ c_{b(k+1)} &= c_{b(k)} - \xi e^{\xi}. \end{aligned} \quad (9)$$

The model  $\mathcal{D}_4$ , is implemented in a Bayesian estimation framework. In this work, we implement the dynamic tracking function as an UKF since the degradation in capacitance (state) due to decrease in electrolyte is considered to be a dynamic non-linear model since evaporation rate ( $j_{eo}$ ) and capacitance oxide breakdown factor ( $c_b$ ) are estimated online based on the state values.

The following steps are implemented for model  $\mathcal{D}_4$ :

1. State Estimation: The current measured capacitance ( $C$ ) is defined as the state variable to be estimated respectively for each of the model and the degradation model is expressed as a discrete time dynamic model in order to estimate current capacitance ( $C$ ) due to decrease in electrolyte volume at the next available measurement. Direct measurements of the capacitance ( $C$ ) is assumed for the filter.
2. Health state forecasting: It is necessary to forecast the state variable once there are no more measurements available at the end of step 1. This is done by evaluating the degradation model through time using the state estimate at time  $t_p$  as initial value.
3. Remaining useful life computation: RUL is computed as the time between time of prediction  $t_p$  and the time at which the forecasted state crosses a certain failure threshold value or EOL.

These steps are repeated for different aging time ( $t_p$ ) through the life of the capacitor device under test. In this work we only consider the model noise and the noise variance as discussed earlier. But for the prediction step we present the means for all the EOL/RUL predictions in our results since the focus of this work is more on deriving the physics-based degradation, implementing it in a Bayesian framework and for prognostics predictions.

### C. UKF for Capacitance State Estimation

The state variable  $\mathbf{x}_k$  (Capacitance) at time  $t_k$  is defined as the current measured capacitance  $C_k$ . Since the system measurements are capacitance ( $C$ ) as well, the output equation is given by  $\mathbf{y}_k = H_k \mathbf{x}_k$ , where  $H$  is the identity matrix. The following system structure is implemented for filtering and prediction using a UKF.

$$\begin{aligned} \mathbf{x}_k &= A_k \mathbf{x}_{k-1} + B_k u + v, \\ \mathbf{y}_k &= H_k \mathbf{x}_k + \mathbf{w}. \end{aligned} \quad (10)$$

where,

$$\begin{aligned} A &= 1, \\ B &= -\frac{(2\epsilon_R \epsilon_0 w_e A_s j_{eo} c_b)}{d_C^2} \Delta t, \\ H &= 1, \\ u &= j_{eo}, c_b. \end{aligned} \quad (11)$$

In this work and application of UKF, the time increment between measurements  $\Delta t$  is not constant since measurements were taken at nonuniform time intervals i.e., the capacitors were characterized at different time intervals. This implies that some of the parameters of the model in Eqn. (14) will change as time progresses. Furthermore,  $v$  and  $w$  are normal random variables with zero mean and  $Q$  and  $R$  variance respectively. The model noise (process noise) variance  $Q$  was estimated from the model regression residuals and was used for the model noise in the Kalman filter implementation. The measurement noise variance  $R$ , was computed from the direct measurements of the capacitance with the EIS equipment, the observed variance is  $4.99 \times 10^{-7}$ . A detailed description of the algorithm implemented in this work can be found in <sup>33</sup>, a description of how the algorithm is used for forecasting can be found in <sup>34</sup> and an example of its usage for prognostics can be found in <sup>19</sup>.

#### D. ESR Degradation Dynamic Model

The complete discrete time dynamic model for  $ESR$  from Eqn. (6) degradation can be summarized as :

$$\mathcal{D}_5 : \frac{1}{ESR_{k+1}} = \frac{1}{ESR_k} - \frac{2w_e A_s j_{eo}}{\rho_E P_E d_C^2 e_b} \Delta t, \quad (12)$$

$$e_{b(k+1)} = e_{b(k)} - \xi.$$

In model  $\mathcal{D}_5$  the rate of evaporation  $j_{eo}$  and the correlation factor,  $P_E$  related to electrolyte spacer porosity and average liquid pathway are the two time-varying parameters. Rate of evaporation,  $j_{eo}$  and resistance dependence oxide breakdown factor,  $e_b$  are the two parameters in the model which are estimated online based on the state variable value,  $ESR$ . Similar steps as followed for model  $\mathcal{D}_5$  as explained earlier for model  $\mathcal{D}_4$ .

#### E. UKF for ESR State Estimation

The state variable  $x_k$  (ESR) at time  $t_k$  is defined as the current measured capacitance  $ESR_k$ . Since the system measurements are  $ESR$  measured values as well, the output equation is given by  $y_k = P_k x_k$ , where  $P$  is the identity matrix. The following system structure is implemented for filtering and prediction using a UKF.

$$\begin{aligned} \mathbf{x}_k &= A_k \mathbf{x}_{k-1} + B_k u + \mathbf{v}, \\ \mathbf{y}_k &= P_k \mathbf{x}_k + \mathbf{w}. \end{aligned} \quad (13)$$

where,

$$\begin{aligned} A &= 1, \\ B &= -\frac{2w_e A_s j_{eo}}{\rho_E P_E d_C^2 e_b} \Delta t, \\ P &= 1, \\ u &= j_{eo}, e_b. \end{aligned} \quad (14)$$

## VII. Prediction of Remaining Useful Life Results and Validation Tests

This section discusses the remaining useful life predictions and validation results using the Alpha-Lambda prognostics metric for the derived degradation models  $\mathcal{D}_4$ , capacitance and  $\mathcal{D}_5$ , ESR respectively. These models were used for making RUL predictions for two different experimental data sets using similar type of capacitors. The discussions in the results and later complete one of our major goals to derive and validate generalized degradation models for electrolytic capacitors.

RUL can be estimated based on the derived physics-based degradation model till the EOL threshold of the device has reached. In the experiments conducted, all the capacitors under test did not reach EOL. The latest characterization reading for degradation in capacitance and ESR parameters was considered as the EOL for calculating the relative accuracy.

#### A. Results for capacitance degradation model ( $\mathcal{D}_4$ )

In this section we discuss the RUL prediction and Validation tests for the capacitance degradation model in the 15V EOS experiment. State estimation and RUL prediction results are discussed for capacitor Cap # 2 out of a batch of 6 available capacitors under test.

Figure 7 shows the result of the filter tracking for completed degradation in capacitance computed upto 200 hours of aging time. The tolerance for the type of electrolytic capacitor under test is approx 15% and hence from the output errors it can be observed that the tracking of the model with respect to the data is acceptable.

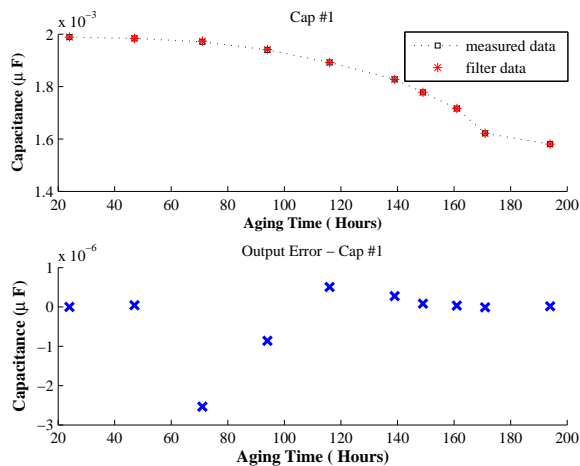


Figure 7. Tracking filter output against measurement data for Cap # 2

### 1. RUL

Figure 8 presents results from the remaining useful life prediction algorithm at different aging times  $t_p = 24, 47, 94, 149, 171$  (hrs), at which the capacitors are characterized and their  $ESR$  value is calculated. The experiments were run till almost 200 hours and hence the predictions are done till the end of experiments. End of life (EOL) is defined as the time at which the forecasted capacitance value trajectory crosses the EOL threshold. Therefore, RUL is EOL minus aging times calculated at  $t_p = 24, 47, 47, 94, 149, 171$  (hrs).

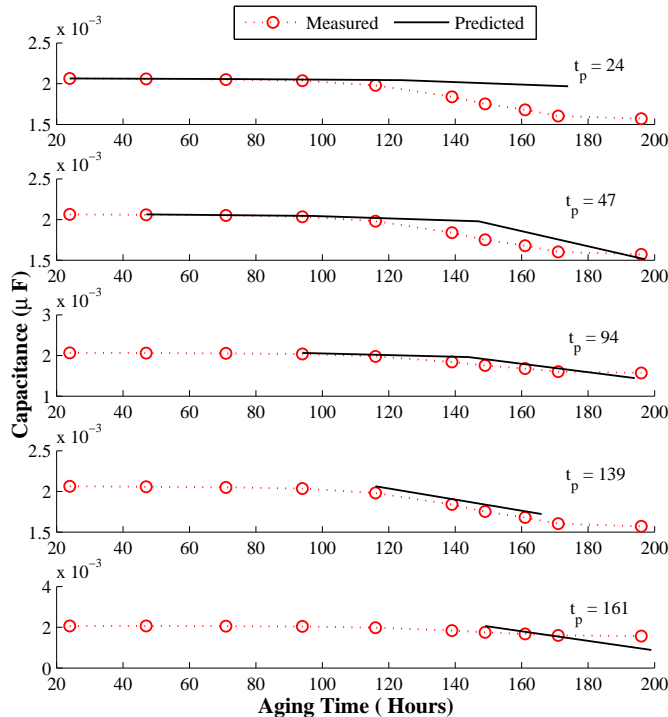
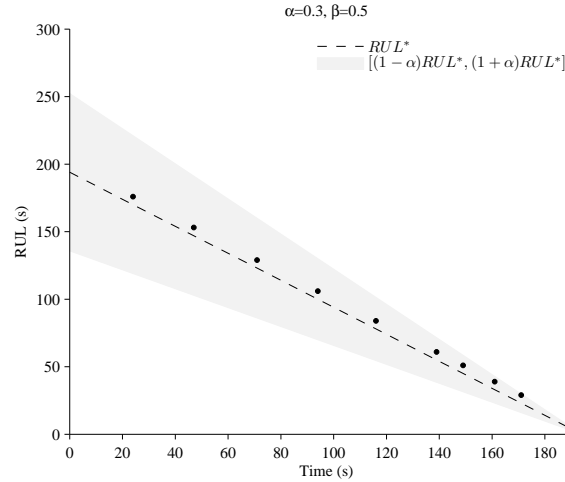


Figure 8. Capacitance decrease prediction at different Aging Time for Cap # 2

## 2. Validation tests



**Figure 9. Performance based on  $\alpha - \lambda$  metric for Cap#2**

An Alpha - Lambda prognostics performance metric<sup>35</sup> is presented in Figure 9 for test case of Cap #2. Performance metric identifies whether the algorithm performs within desired error margins (specified by the parameter  $\alpha$ ) of the actual RUL at any given time instant (specified by the parameter  $\lambda$ ).<sup>35</sup> The central dashed line represents ground truth and the shaded region corresponds to a 30% ( $\alpha = 0.3$ ) error bound in the RUL prediction. From the metric plot in Figure 9 we note that the relative accuracy remains high till the end of the RUL prediction period. As mentioned earlier this can be attributed to the accuracy of the model, and the state-based tracking approach, where the state is updated as new data points become available.

**Table 1. Validation results based on RA for Capacitance degradation model  $\mathcal{D}_4$  - 15V**

Aging Time	C1	C2	C3	C4	C5	C6	$\overline{RA}_a$
24	98.85	98.27	98.85	97.67	98.27	96.47	98.06
47	98.68	98.00	98.68	97.32	98.00	95.92	97.76
71	98.43	97.62	98.43	96.80	97.62	95.12	97.34
94	98.08	97.09	98.08	96.08	97.09	94.00	96.73
116	97.56	96.30	97.56	95.00	96.30	92.31	95.84
139	96.61	94.83	96.61	92.98	94.83	89.09	94.16
149	95.92	93.75	95.92	91.49	93.75	86.67	92.92
161	94.59	91.67	94.59	88.57	91.67	81.82	90.49
171	92.59	88.46	92.59	84.00	88.46	73.91	86.67
$\overline{RA}_b$	96.81	95.11	96.81	93.32	95.11	89.48	

$\overline{RA}_a$  is the mean relative accuracy of all capacitors at each prediction time ( $t_p$ )

$\overline{RA}_b$  is the mean relative accuracy of each capacitor at all prediction times

### B. Results for ESR degradation model ( $\mathcal{D}_5$ )

State estimation and RUL prediction results are discussed for capacitor Cap #2. Figure 10 shows the result of the filter tracking for completed degradation in capacitance upto 200 hours of aging time. As can be observed from the residuals the tracking of the model with respect to the data is acceptable.

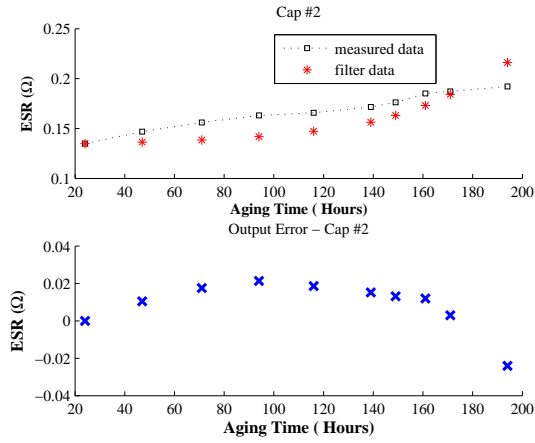


Figure 10. Tracking filter output against measurement data for Cap # 2

### 1. RUL

Figure 11 presents results from the remaining useful life prediction algorithm at different aging times  $t_p = 24, 47, 94, 149, 171$  (hrs), at which the capacitors are characterized and their  $ESR$  value is calculated. Model  $\mathcal{D}_5$  is implemented for predicting the increase in  $ESR$  while the measured values are the  $ESR$  measurements done at respective aging time intervals. The experiments were run till almost 200 hours and hence the predictions are done till the end of experiments. End of life (EOL) is defined as the time at which the forecasted capacitance value trajectory crosses the EOL threshold at end of 200 hrs. Therefore, RUL is EOL minus aging times  $t_p = 24, 47, 94, 149, 171$  (hrs).

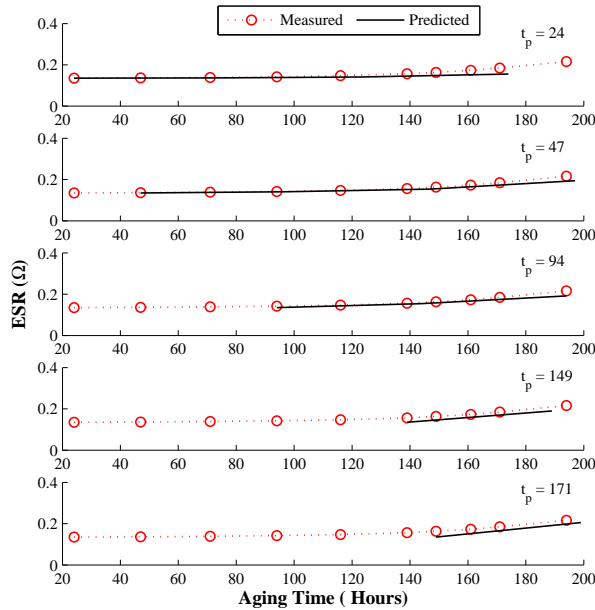


Figure 11. ESR prediction at different Aging Time for Cap # 2 by Model  $\mathcal{D}_5$

### 2. Validation tests

An  $\alpha$ - $\lambda$  prognostics performance metric is presented in Figure 12 for test case of Cap #2. The central dashed line represents ground truth and the shaded region is corresponding to a 30% ( $\alpha = 0.3$ ) error bound in the RUL prediction.

From the  $\alpha$ - $\lambda$  metric plot in Figure 12 it can be observed that the relative accuracy is good till the end of the experiment time and the accuracy is good enough under acceptable limits. As mentioned earlier this is due to inclusion of the degradation parameters and estimating them as the  $ESR$  increases with degradation.

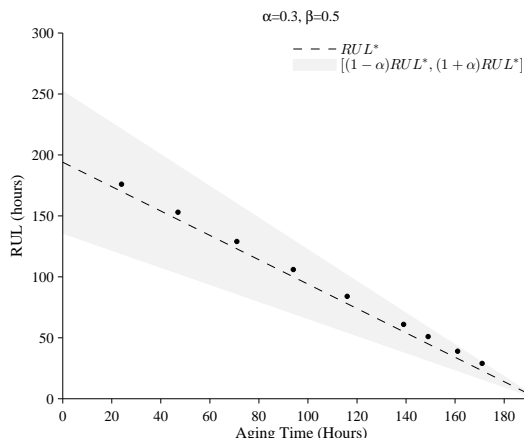


Figure 12. Performance based on Alpha-Lambda metric for Cap#2

Table 2. Summary of validation results based on RA for ESR degradation model  $\mathcal{D}_5$  - 15V

Aging Time	C1	C2	C3	C4	C5	C6	$\overline{RA}_a$
24	96.47	96.47	96.47	96.47	96.47	96.47	96.47
47	95.92	95.92	95.92	95.92	95.92	95.92	95.92
71	95.12	95.12	95.12	95.12	95.12	95.12	95.12
94	94.00	94.00	94.00	94.00	94.00	94.00	94.00
116	92.31	92.31	92.31	92.31	92.31	92.31	92.31
139	89.09	89.09	89.09	89.09	89.09	89.09	89.09
149	86.67	86.67	86.67	86.67	86.67	86.67	86.67
161	81.82	81.82	81.82	81.82	81.82	81.82	81.82
171	73.91	73.91	73.91	73.91	73.91	73.91	73.91
$\overline{RA}_b$	89.48	89.48	89.48	89.48	89.48	89.48	

$\overline{RA}_a$  is the mean relative accuracy of all capacitors at each prediction time ( $t_p$ )

$\overline{RA}_b$  is the mean relative accuracy of each capacitor at all prediction times

## VIII. Conclusion and Discussion

The results presented here are based on accelerated aging experimental data and on the accelerated life timescale. This paper presents a first principles based degradation electrolytic capacitor model and an parameter estimation algorithm to validate the derived model, based on the experimental data. When comparing the results generated by the capacitance empirical model<sup>20,31</sup> in our previous work, the physics-based degradation model in table 1, we note that the accuracy of the two models are comparable initially, but the empirical model results degrade toward the end of capacitor life. This is primarily because a simple linear first-order model with static parameter values is employed for tracking the capacitor degradation.

Physics-based model  $\mathcal{D}_4$  for capacitance more accurately represents the actual degradation phenomena because it includes the first principles operation parameters like evaporation rate, break down rate, device geometry etc. The use of the UKF allows for more accurate tracking as compared to an Kalman filter, especially when the behaviors are nonlinear in the later stages of the aging cycle. The tuning and estimation of parameters in the empirical model using UKF is relatively simpler and also computationally less expensive. On the other-hand, in UKF the parameters

are tuned online as updated data is received and hence computationally expensive. Similarly the degradation model  $D_5$  for *ESR* based on the first principles gives an indication of how a specific device degrades based on its structure, material properties, operating conditions, etc. which results in better prediction accuracy for RUL.

Overall both models have their own advantages and disadvantages. The comparison of the two models and prediction results can help us decide which models to implement based on the requirements. If the model needs to be simpler and computationally less expensive then the empirical model can be implemented where the model prediction accuracy will be compromised while if accuracy is more important then a complex model and computationally expensive methodology can be implemented. Further research will focus on development of functional mappings that will translate the accelerated life timescale into real usage conditions timescale, where the degradation process dynamics will be slower, and subjected to varying stress conditions.

## Acknowledgments

This work was funded by the NASA Aviation Safety Program, IVHM and SSAT projects and NRA grant # NNX07ADIZA.

## References

- <sup>1</sup>Vichare, N. and Pecht, M., "Prognostics and Health Management of Electronics," *IEEE Transactions on Components and Packaging Technologies*, Vol. Vol 29, 2006, pp. 222 – 229.
- <sup>2</sup>FIDESGroup, "Reliability Methodology for Electronic Systems," *FIDES Guide issue A*, 2004.
- <sup>3</sup>Celaya, J., Wysocki, P., Vashchenko, V., Saha, S., and Goebel, K., "Accelerated aging system for prognostics of power semiconductor devices," *Proceedings of IEEE Autotestcon*, September 2010, pp. 1–6.
- <sup>4</sup>Ferrell, B. L., "JSF Prognostics and Health Management," *IEEE Aerospace Conference*, 1999.
- <sup>5</sup>Balaban, E., Saxena, A., Narasimhan, S., Roychoudhury, I., Goebel, K., and Koopmans, M., "Airborne Electro-Mechanical Actuator Test Stand for Development of Prognostic Health Management Systems," *Proceedings of Annual Conference of the PHM Society 2010, October 10-16, Portland, OR*, 2010.
- <sup>6</sup>Goodman, D., "Practical Application of PHM/Prognostics to COTS Power Converters," *Aerospace Conference, 2005 IEEE*, March 2005, pp. 3573 – 3578.
- <sup>7</sup>Pecht, M., Dube, M., Natishan, M., and Knowles, I., "An Evaluation of Built-In Test," *IEEE Transactions on Aerospace and Electronic Systems*, Vol. 37, 2001, pp. 266 – 272.
- <sup>8</sup>Johnson, D., "Review of Fault Management Techniques Used in Safety Critical Avionic Systems," *Progress in Aerospace Science*, Vol. 31, October 1996, pp. 415 – 431.
- <sup>9</sup>Leonard, C. and Pecht, M. G., "Improved techniques for cost effective electronics," *Proceedings of Reliability Maintainability Symposium*, 1991, pp. 174 – 182.
- <sup>10</sup>Judkins, J. B., Hofmeister, J., and Vohnout, S., "A Prognostic Sensor for Voltage Regulated Switch-Mode Power Supplies," *IEEE Aerospace Conference*, Vol. 1, 2007, pp. 1 – 8.
- <sup>11</sup>Orsagh, R. and et'al, "Prognostic Health Management for Avionics System Power Supplies," *Aerospace Conference, 2006 IEEE*, March 2006, pp. 1 – 7.
- <sup>12</sup>Nie, L., Azarian, M., Keimasi, M., and Pecht, M., "Prognostics of ceramic capacitor temperature humidity bias reliability using mahalanobis distance," *Circuit World*, Vol. 33(3), 2007, pp. 21 – 28.
- <sup>13</sup>Gu, J. and Pecht, M., "Prognostics and Health Management Using Physics-of-Failure," *54th Annual Reliability and Maintainability Symposium (RAMS)*, 2008.
- <sup>14</sup>Wereszczak, A., Breder, K., and Ferber, M. K., "Failure Probability Prediction of Dielectric Ceramics in Multilayer Capacitors," *Annual Meeting of the American Ceramic Society, Cincinnati, OH (United States)*, 1998.
- <sup>15</sup>Buiatti, G., Martin-Ramos, J., Garcia, C., Amaral, A., and Cardoso, A., "An Online and Noninvasive Technique for the Condition Monitoring of Capacitors in Boost Converters," *IEEE Transactions on Instrumentation and Measurement*, Vol. 59, 2010, pp. 2134 – 2143.
- <sup>16</sup>Imam, A. M., Habetler, T., Harley, R., and Divan, D., "Condition Monitoring of Electrolytic Capacitor in Power Electronic Circuits using Adaptive Filter Modeling," *IEEE 36th Power Electronics Specialists Conference, 2005. PESC '05.*, June 2005, pp. 601 – 607.
- <sup>17</sup>Hansen, P. and McCluskey, P., "Failure models in power device interconnects," *European Conference on Power Electronics and Applications*, 2007, pp. 1 – 9.
- <sup>18</sup>Upadhyayula, K. and Dasgupta, A., "Guidelines for Physics-of-Failure Based Accelerated Stress Testing," *Annual Reliability and Maintainability Symposium*, 1998, pp. 345 – 357.
- <sup>19</sup>Daigle, M., Saha, B., and Goebel, K., "A Comparison of Filter-based Approaches for Model-based Prognostics," *Proceedings of the 2012 IEEE Aerospace Conference*, March 2012.
- <sup>20</sup>Celaya, J., Kulkarni, C., Goebel, K., and Biswas, G., "Prognostic Studies and Physics of failure modeling under High Electrical Stress for Electrolytic Capacitors," *International Journal of Prognostics and Health Management*, Vol. 3(2), 2012, pp. 1 – 18.
- <sup>21</sup>Kulkarni, C., Biswas, G., Celaya, J., and Goebel, K., "Physics Based Degradation Models for Capacitor Prognostics under Thermal Overtress Conditions," *International Journal of Prognostics and Health Management*, Vol. 4(1), 2013, pp. 1 – 21.
- <sup>22</sup>Lahyani, A., Venet, P., Grellet, G., and Viverge, P., "Failure prediction of electrolytic capacitors during operation of a switchmode power supply," *IEEE Transactions on Power Electronics*, Vol. 13, Nov 1998, pp. 1199 – 1207.

- <sup>23</sup>Eliasson, L., "Aluminium Electrolytic Capacitor's performance in Very High Ripple Current and Temperature Applications," *CARTS Europe 2007 Symposium, Spain*, October - November 2007.
- <sup>24</sup>Luo, J., Namburu, M., Pattipati, K., and et'al, "Model-based Prognostic Techniques," *AUTOTESTCON 2003. IEEE Systems Readiness Technology Conference. Proceedings*, Sep 2003, pp. 330 – 340.
- <sup>25</sup>Wit, H. D. and Crevecoeur, C., "The dielectric breakdown of anodic aluminum oxide," *Physics Letters A*, Vol. Volume 50, Issue 5, 1974, pp. 365 – 366.
- <sup>26</sup>Rusdi, M., Moroi, Y., Nakahara, H., and Shibata, O., "Evaporation from Water Ethylene Glycol Liquid Mixture," *Langmuir - American Chemical Society*, Vol. 21 (16), 2005, pp. 7308 – 7310.
- <sup>27</sup>Rodner, S. C., Wedin, P., and Bergstram, L., "Effect of Electrolyte and Evaporation Rate on the Structural Features of Dried Silica Monolayer Films," *Langmuir*, Vol. 18, No. 24, 2002, pp. 9327 – 9333.
- <sup>28</sup>Bengt, A., "Electrolytic Capacitors Theory and Applications," *RIFA Electrolytic Capacitors*, 1995.
- <sup>29</sup>Tasca, D. M., "Pulse Power Response and Damage Characterization of Capacitors," *Electrical Overstress-Electrostatic Discharge Symposium Proceedings, EOS/ESD Association*, Vol. 3, 1981.
- <sup>30</sup>Kadary, V. and Klein, N., "Electrical Breakdown: I. During the Anodic Growth of Tantalum Pentoxide," *The Journal of the Electrochemical Society*, Vol. 127, 1980, pp. 139 – 151.
- <sup>31</sup>Kulkarni, C., Celaya, J., Goebel, K., and Biswas, G., "Prognostics Health Management and Physics based failure Models for Electrolytic Capacitors," *Proceedings of American Institute of Aeronautics and Astronautics, AIAA Infotech Aerospace Conference, Garden Grove, CA*, June 2012, pp. 1 – 8.
- <sup>32</sup>Julier, S. J. and Uhlmann, J. K., "Unscented filtering and nonlinear estimation," *Proceedings of the IEEE*, Vol. 92, No. 3, 2004, pp. 401 – 422.
- <sup>33</sup>Stengel, R., *Optimal Control and Estimation*, Dover Books on Advanced Mathematics, 1994.
- <sup>34</sup>Chatfield, C., *The Analysis of Time Series: An Introduction*, Chapman & Hall/CRC, 2003.
- <sup>35</sup>Saxena, A., Celaya, J., Saha, B., Saha, S., and Goebel, K., "On Applying the Prognostic Performance Metrics," *Annual Conference of the Prognostics and Health Management Society*, September 2009.